

Received October 5, 2017, accepted November 6, 2017, date of publication November 14, 2017, date of current version December 5, 2017.

Digital Object Identifier 10.1109/ACCESS.2017.2772302

Minimum Symbol-Error Rate Based Adaptive Decision Feedback Equalizer in Underwater Acoustic Channels

FANGJIONG CHEN¹, (Member, IEEE), SHAOE LIN¹, BEIXIONG ZHENG¹, QIANG LI¹, MIAOWEN WEN¹, (Member, IEEE), YUN LIU^{1,2}, AND FEI JI¹, (Member, IEEE)

¹School of Electronic and Information Engineering, South China University of Technology, Guangzhou 510641, China

²School of Information Science and Technology, Zhongkai University of Agriculture and Engineering, Guangzhou 510225, China

Corresponding author: Beixiong Zheng (zheng.bx@mail.scut.edu.cn)

This work was supported in part by the National Natural Science Foundation of China under Grant 61671211, Grant 61431005, and Grant 61501531 and in part by the Natural Science Foundation of Guangdong Province under Grant 2016A030311024 and Grant 2015A030313602.

ABSTRACT Adaptive linear equalizer, whose coefficients are designed to be adjustable to the channel impulse response, has emerged as a simple and efficient technique to adaptively compensate for the channel fading. However, conventional adaptive linear equalizers suffer from performance degradation and slow convergence in the underwater acoustic channel with large delay spread. To solve this problem, in this paper, we propose a novel adaptive decision-feedback equalizer (DFE) based on the minimum symbol-error rate (MSER) criterion. Specifically, by taking the sample-by-sample adaptation into account, the problem is first formulated as minimizing the norm between two consecutive adaptations under the constraint that the latest adaptation will provide correct detection for both the current and past symbols. Then we solve the optimization problem by using the Lagrange multiplier method to obtain the adaptive DFE that minimizes the sequential symbol detection error with a fast convergence rate. Simulation results show that the proposed MSER-based adaptive DFE significantly outperforms the existing equalizers in terms of convergence speed and steady-state performance for underwater acoustic channels.

INDEX TERMS Minimum symbol-error rate (MSER), decision-feedback equalizer, channel equalization, underwater acoustic channel, Lagrange multiplier.

I. INTRODUCTION

Underwater acoustic communications have shown broad prospects and received great interest in many fields, such as ocean image transmission, marine disasters detection, underwater navigation, and marine environmental monitoring [1]–[3]. However, underwater acoustic channel is one of the most challenging wireless communication media. Underwater acoustic channel is highly selective and has large multipath delay spread of tens or hundreds of milliseconds, resulting in severe frequency-selective signal distortion. Specifically, due to the low propagation speed at 1500m/s of acoustic waves, multipath spread leads to long-time delay characteristic of the underwater acoustic channels and severe inter-symbol interference (ISI) when received signals from different delay paths are superimposed with each other [4]–[6].

Linear finite impulse response (FIR) equalizers are widely applied in many scenarios owing its simple structure and

low computational complexity. It is worth pointing out that the length of the linear equalizer is typically larger than the maximum delay spread of the channel [7], [8]. Therefore, for channels with large delay spread, linear equalizer of high order should be applied to compensate the channel effect appropriately. However, linear equalizer of extremely high order, e.g. more than 100, becomes less impressive in practical system as it suffers from slow convergence and poor error performance [9]. One kind of simple but efficient nonlinear equalizer, namely the adaptive decision-feedback equalizer (DFE), has been considered as a promising technique to tackle the above-mentioned difficulty. The adaptive DFE consists of a feedforward filter and a feedback filter, whose coefficients will adjust recursively to track the CIR and compensate the channel effect. The basic idea lied in DFE is that once the symbols are successfully detected, the residual ISI at the output of the forward equalizer can be estimated and subtracted by using those past detected symbols.

The DFE has been applied in various channels with large delay spread, such as ADSL channels [10], underwater acoustic channel [11], [12], and terrestrial wireless channels [13], which has been shown to be more efficient than conventional linear adaptive equalizers. Moreover, for coded systems, the system performance can be improved by using the decoded symbols as the feedback to the DFE [14], [15].

Usually the DFEs are designed based on the minimum mean-square-error (MMSE) principle, as this leads to the effective adaptive implementation in the form of the LMS algorithm. The MMSE criterion intends to minimize the mean-square-error between the equalizer output and the target signal. However, it has been illustrated by various simulations that minimizing the mean-square-error does not necessarily achieve the minimum symbol-error rate (MSER) performance [16]–[18]. Designing channel equalizer directly based on the MSER criterion has attracted significant attention [16]–[22]. In the existing work, the MSER criterion has been applied to design the DFE [20]–[22]. However, the existing MSER-based DFEs are derived from the symbol-error rate (SER) objective function, which is non-convex and has an extremely complicated expression. As a consequence, the resulting equalizers usually have complicated structure, which are not suitable to apply in practical communication systems. Moreover, those DFEs in [20]–[22] involve a prior knowledge of the CIR and noise variance. In practical communication systems, however, such information is difficult to obtain or even unavailable, especially for underwater acoustic channels. Moreover, existing MSER-based equalizers only work well with low order (less than 10) and often lose their advantages with high order. Therefore, the MSER-based equalizer applied for underwater acoustic channels remains an open as well as challenging research problem.

To fill the aforementioned gap, in this paper we investigate the fast convergent equalization based on the MSER criterion under channels with the maximum delay spread more than 100 symbol periods. Specifically, we consider the sample-by-sample adaptive equalizer in the single-carrier system, where the coefficients of the equalizer are updated whenever a new sample arrives. The problem for the adaptive MSER-based equalization is then formulated as minimizing the norm between two consecutive adaptations under the constraint that the new adaptation would provide correct symbol detection. By applying the Lagrange multiplier method to the constrained optimization problem, we then derive a novel adaptive DFE with recursive structure, tailored to underwater acoustic channels. Simulations over typical underwater acoustic channels show that the proposed adaptive DFE converges significantly faster and achieves much better steady-state error performance than the existing equalizers with linear or decision feedback structure.

The rest of this paper is organized as follows. Section II describes the signal models for the channel and equalizer. In Section III, we propose the adaptive DFE based on the MSER criterion with recursive structure. Section IV presents the simulation results for different equalizers over underwater

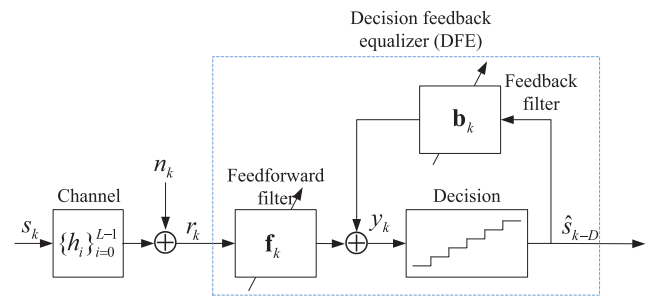


FIGURE 1. Block diagram of channel, DFE, and memoryless decision device.

acoustic channels. Finally, we summarize our results and draw conclusion in Section V.

II. SYSTEM MODEL AND EQUALIZATION

The block diagram of the discrete-time system is shown in Fig. 1. After the multi-path channel with different delay spreads, the received signal at the k -th time slot is given by

$$r_k = \sum_{i=0}^{L-1} h_i s_{k-i} + n_k \quad (1)$$

where s_k denotes the modulation symbol independently drawn from a complex alphabet, $\{h_i\}_{i=0}^{L-1}$ denote the CIR with L being the maximum delay spread of the channel, n_k represents the additive white Gaussian noise (AWGN) with zero mean and variance σ^2 . It can be observed from (1) that the channel with delay spread gives rise to ISI, which implies that the received signal over a given symbol period experiences interference from other symbols that have been delayed by multipath.

To mitigate the ISI due to the delay spread of the channel, a class of simple and nonlinear equalizers termed as the adaptive DFE, which consists of a feedforward filter and a feedback filter, can be implemented at the receiver to reverse the channel dispersion effect effectively. Specifically, the output of the DFE at the k -th time slot can be represented by a linear combination of the received samples and past detected symbols:

$$y_k = \mathbf{f}_k^T \mathbf{r}_k + \mathbf{b}_k^T \hat{\mathbf{s}}_k \quad (2)$$

where $\mathbf{f}_k = [f_{k,0}, f_{k,1}, \dots, f_{k,N_f-1}]^T$ is an $N_f \times 1$ vector that represents the feedforward filter, $\mathbf{b}_k = [b_{k,0}, b_{k,1}, \dots, b_{k,N_b-1}]^T$ is an $N_b \times 1$ vector that represents the feedback filter, $\mathbf{r}_k = [r_k, r_{k-1}, \dots, r_{k-N_f+1}]^T$ represents an $N_f \times 1$ received signal vector consisting of N_f consecutive received samples, $\hat{\mathbf{s}}_k = [\hat{s}_{k-D-1}, \hat{s}_{k-D-2}, \dots, \hat{s}_{k-D-N_b}]^T$ is an $N_b \times 1$ vector consisted of N_b past detected symbols with D being the delay of the equalizer.

Here we consider an uncoded system, where hard decision principle is applied to the output of the DFE. For instance, the estimation of BPSK modulation symbol with delay D is

detected from the output of the DFE, i.e.,

$$\hat{s}_{k-D} = f_{dec}(y_k) = \text{sgn}(y_k) = \begin{cases} +1, & y_k \geq 0 \\ -1, & y_k < 0. \end{cases} \quad (3)$$

According to the MSER principle, we intend to design a MSER-based algorithm that minimizes the symbol error probability directly, i.e., $\min \{\text{Prob}\{s_{k-D} \neq f_{dec}(y_k)\}\}$. Under the sample-by-sample adaptive equalization, the current filter coefficients, i.e., \mathbf{f}_k and \mathbf{b}_k , are updated from the previous filter coefficients \mathbf{f}_{k-1} and \mathbf{b}_{k-1} whenever the new data symbol arrives. In order to achieve fast convergence speed for the training of the equalizer, we formulate the objective function by minimizing the Euclidean distance of the filter coefficients between two consecutive adaptations [19], which can be expressed as

$$\min_{\mathbf{f}_k, \mathbf{b}_k} \left\{ \|\mathbf{f}_k - \mathbf{f}_{k-1}\|^2 + \|\mathbf{b}_k - \mathbf{b}_{k-1}\|^2 \right\}. \quad (4)$$

At the same time, the feedforward filter coupled with the feedback filter is forced to provide the correct symbol detection, so as to minimize the SER. In the following section, we will put forth an effective adaptive DFE with recursive structure to provide correct symbol detection for both the current and the past symbols, in which the constraint is formulated as $\{s_{i-D} = f_{dec}(y_i)\}$ for $i = k, k-1, \dots, D$.

III. MSER-BASED ADAPTIVE DFE

Existing adaptive linear equalizers and DFEs that are based on MSER criterion suffer from slow convergence, especially in the underwater acoustic channel with large delay spread. To accelerate the convergence rate, we explore an adaptive DFE with recursive structure that minimizes the sequential symbol detection error, which tries to provide correct symbol detection not only in the current time slot, but also in the past time slots. For simplicity, we combine the feedforward and feedback filters into a uniform filter vector as $\mathbf{c}_k = [\mathbf{f}_k^T, \mathbf{b}_k^T]^T$ such that the equalizer output can be represented as $y_k = \mathbf{c}_k^T \mathbf{v}_k$, where $\mathbf{v}_k = [\mathbf{r}_k^T, \hat{\mathbf{s}}_k^T]^T$.

A. BPSK SOURCE

We first consider the channel equalization under the premise of BPSK modulation. The constraint of correct symbol detection, including both current and past data symbols, can be formulated as

$$f_{dec}(y_k) = \text{sgn}(\mathbf{c}_k^T \mathbf{v}_i) = \begin{cases} +1, & \text{when } s_{i-D} = +1 \\ -1, & \text{when } s_{i-D} = -1 \end{cases} \quad (5)$$

where $i = k, k-1, \dots, D$ denote both the current and past time slots. With the constraint given in (5), we formulate the optimization problem as

$$\min_{\mathbf{c}_k} \|\mathbf{c}_k - \mathbf{c}_{k-1}\|^2 \quad (6)$$

$$\text{s.t. } \text{sgn}(\mathbf{c}_k^T \mathbf{v}_i) - s_{i-D} = 0 \\ i = k, k-1, \dots, D. \quad (7)$$

To find the fast convergence solution, we apply the Lagrange multiplier method to solve this optimization problem. We first

approximate $\text{sgn}(x)$ with $\tanh(\beta x)$ to make the objective function derivable and formulate the objective function as

$$J(\mathbf{c}_k) = \|\mathbf{c}_k - \mathbf{c}_{k-1}\|^2 + \sum_{i=D}^k \lambda_i (\tanh(\beta \mathbf{c}_k^T \mathbf{v}_i) - s_{i-D}) \quad (8)$$

where $\{\lambda_i\}_{i=D}^k$ are the Lagrange multipliers.

Proposition 1: By setting the partial derivative of $J(\mathbf{c}_k)$ with respect to \mathbf{c}_k to zero, we obtain the following iterative adaptation formula for the MSER-based adaptive DFE:

$$\mathbf{c}_k = \mathbf{c}_{k-1} - \zeta_k \mathbf{R}_k^{-1} \mathbf{v}_k \quad (9)$$

where

$$\zeta_k = \frac{(\tanh(\beta \mathbf{c}_{k-1}^T \mathbf{v}_k) - s_{k-D})}{\beta \tanh'(\beta)} \quad (10)$$

is the error indicator of symbol detection and the correlation matrix \mathbf{R}_k is given by

$$\mathbf{R}_k = \sum_{j=D}^k w^{k-j} (\mathbf{v}_j \mathbf{v}_j^T), \quad (11)$$

with w denoting the forgetting factor.

Proof: See Appendix A. ■

In (11), \mathbf{R}_k can be regarded as the weighted sum of the $(N_f + N_b) \times (N_f + N_b)$ instant autocorrelation matrix $\mathbf{v}_j \mathbf{v}_j^T$. However, directly calculating \mathbf{R}_k^{-1} at each iteration is very inefficient, which will impose high computation to the receiver. To avoid the explicit matrix inversion of \mathbf{R}_k at each iteration, we first calculate the recursive update of \mathbf{R}_k as follows:

$$\mathbf{R}_k = w \mathbf{R}_{k-1} + \mathbf{v}_k \mathbf{v}_k^T. \quad (12)$$

Then, based on the Sherman-Morrison formula [23], the recursive update of \mathbf{R}_k^{-1} can be calculated as

$$\mathbf{R}_k^{-1} = \frac{1}{w} \left[\mathbf{R}_{k-1}^{-1} - \frac{\mathbf{R}_{k-1}^{-1} \mathbf{v}_k \mathbf{v}_k^T \mathbf{R}_{k-1}^{-1}}{w + \mathbf{v}_k^T \mathbf{R}_{k-1}^{-1} \mathbf{v}_k} \right]. \quad (13)$$

To summarize, suppose we have \mathbf{c}_{k-1} and \mathbf{R}_{k-1}^{-1} beforehand. When a new data symbol is received, we have \mathbf{v}_k to be utilized for the update of the filter vector \mathbf{c}_k and the inverse of the correlation matrix \mathbf{R}_k^{-1} according to (9) and (13), respectively. Then the recursive computation for the update of the equalizer \mathbf{c}_k and the inverse of the correlation matrix \mathbf{R}_k^{-1} can be carried out as follows:

- *Step 1:* compute the error indicator of symbol detection ζ_k according to (10);
- *Step 2:* update the inverse of the correlation matrix \mathbf{R}_k^{-1} according to (13);
- *Step 3:* update the equalizer \mathbf{c}_k according to (9).

B. QAM SOURCE

In this subsection, we extend the proposed MSER-based adaptive DFE to QAM source. We assume that the real and imaginary parts of the M -QAM symbols are independently and uniformly drawn from the alphabet of $\{\pm d, \pm 3d, \dots, \pm(\sqrt{M}-1)d\}$, where d denotes half of the distance between any two adjacent constellation points. Moreover, as the real and imaginary parts of the modulation symbols are independently generated, the real and imaginary parts of the equalizer output can be separately detected. Hereafter we drop the time index for notational simplicity. Let us take the real part of the equalizer output as an illustrative case, which can be expressed as

$$\Re\{y_k\} = \Re\{\mathbf{c}_k^T \mathbf{v}_k\} = \mathbf{c}_R^T \mathbf{v}_R - \mathbf{c}_I^T \mathbf{v}_I = \bar{\mathbf{c}}_k^T \bar{\mathbf{v}}_k \quad (14)$$

where $\mathbf{c}_R, \mathbf{c}_I$ and $\mathbf{v}_R, \mathbf{v}_I$ are the real and imaginary parts of the filter \mathbf{c}_k and input signal \mathbf{v}_k , respectively, and we denote $\bar{\mathbf{c}}_k = [\mathbf{c}_R^T, -\mathbf{c}_I^T]^T, \bar{\mathbf{v}}_k = [\mathbf{v}_R^T, \mathbf{v}_I^T]^T$.

Based on the MSER criterion, $\bar{\mathbf{c}}_k$ is designed to minimize $\text{Prob}\{\Re\{s_{i-D}\} \neq f_{dec}(\Re\{y_i\})\}$ for $i = k, k-1, \dots, D$ regardless of the imaginary part. Considering the multiple constraints, we formulate the optimization problem as

$$\min_{\bar{\mathbf{c}}_k} \|\bar{\mathbf{c}}_k - \bar{\mathbf{c}}_{k-1}\|^2 \quad (15)$$

$$\text{s.t. } \left| \Re\{\bar{\mathbf{c}}_k^T \bar{\mathbf{v}}_i\} - \Re\{s_{i-D}\} \right| < d \quad (16)$$

$$i = k, k-1, \dots, D.$$

The constraints in (16) imply that the currently updated equalizer coefficients, i.e., $\bar{\mathbf{c}}_k$, should provide correct detection for both the current and past symbols. The constraints in (16) can be equivalently expressed as

$$\text{sgn}\left(\bar{\mathbf{c}}_k^T \bar{\mathbf{v}}_i - \Re\{s_{i-D}\} + d\right) + \text{sgn}\left(\bar{\mathbf{c}}_k^T \bar{\mathbf{v}}_i - \Re\{s_{i-D}\} - d\right) = 0 \quad (17)$$

where $i = k, k-1, \dots, D$. After replacing $\text{sgn}(x)$ with $\tanh(\beta x)$, we obtain the following objective function based on the Lagrange multiplier method, which is formulated as

$$J(\bar{\mathbf{c}}_k) = \|\bar{\mathbf{c}}_k - \bar{\mathbf{c}}_{k-1}\|^2 + \sum_{i=D}^k \lambda_i \left(\tanh\left(\beta(\bar{\mathbf{c}}_k^T \bar{\mathbf{v}}_i - \Re\{s_{i-D}\} + d)\right) + \tanh\left(\beta(\bar{\mathbf{c}}_k^T \bar{\mathbf{v}}_i - \Re\{s_{i-D}\} - d)\right) \right) \quad (18)$$

where $\{\lambda_i\}_{i=D}^k$ denote the Lagrange multipliers.

Proposition 2: After setting the derivative of $J(\bar{\mathbf{c}}_k)$ with respect to $\bar{\mathbf{c}}_k$ to zero, we can obtain the following adaptive equation:

$$\bar{\mathbf{c}}_k = \bar{\mathbf{c}}_{k-1} - \Re\{\zeta_k\} \bar{\mathbf{R}}_k^{-1} \bar{\mathbf{v}}_k \quad (19)$$

where

$$\Re\{\zeta_k\} = \frac{\tanh(\beta(\Omega_R + d)) + \tanh(\beta(\Omega_R - d))}{2\beta \tanh'(\beta)} \quad (20)$$

with $\Omega_R = \bar{\mathbf{c}}_{k-1}^T \bar{\mathbf{v}}_k - \Re\{s_{k-D}\}$ denoting the real part of the bias of the equalizer output.

Proof: See Appendix B. ■

Taking the imaginary part of the equalizer output into account, we have

$$\Im\{y_k\} = \Im\{\mathbf{c}_k^T \mathbf{v}_k\} = \mathbf{c}_R^T \mathbf{v}_I + \mathbf{c}_I^T \mathbf{v}_R = \bar{\mathbf{c}}_k^T \mathbf{P} \bar{\mathbf{v}}_k \quad (21)$$

where \mathbf{P} is a permutation matrix given by

$$\mathbf{P} = \begin{bmatrix} 0 & \mathbf{I}_{N_f+N_b} \\ -\mathbf{I}_{N_f+N_b} & 0 \end{bmatrix}$$

with $\mathbf{I}_{N_f+N_b}$ being an $(N_f + N_b) \times (N_f + N_b)$ identity matrix. After the similar derivations to that for the real part in (19), we obtain the following update equation for the imaginary part of the equalizer output:

$$\bar{\mathbf{c}}_k = \bar{\mathbf{c}}_{k-1} - \Im\{\zeta_k\} \bar{\mathbf{R}}_k^{-1} \mathbf{P} \bar{\mathbf{v}}_k \quad (22)$$

where

$$\Im\{\zeta_k\} = \frac{\tanh(\beta(\Omega_I + d)) + \tanh(\beta(\Omega_I - d))}{2\beta \tanh'(\beta)} \quad (23)$$

with $\Omega_I = \bar{\mathbf{c}}_{k-1}^T \mathbf{P} \bar{\mathbf{v}}_k - \Im\{s_{k-D}\}$ representing the imaginary part of the bias of the equalizer output. Combining the real part with the imaginary part of the equalizer output leads to the following complex version of the MSER-based adaptive DFE:

$$\mathbf{c}_k = \mathbf{c}_{k-1} - \zeta_k \mathbf{R}_k^{-1} \mathbf{v}_k^* \quad (24)$$

The recursive computation for the update of the equalizer \mathbf{c}_k and the inverse of the correlation matrix \mathbf{R}_k^{-1} can follow the same steps as given in the previous subsection.

IV. SIMULATION RESULTS

In this section, simulation results are presented to demonstrate the effectiveness of the proposed algorithm, where underwater acoustic channels are considered. Both statistical channel model and real-world communication channels are considered in the simulations. The statistical channel model is from [24], and the real communication channels are measured from experimental underwater acoustic communication tests. The received signal-to-noise-ratio (SNR) is defined as $\text{SNR} = 10 \log_{10} \left[E_s \cdot \sum_{i=0}^L h_i^2 / \sigma^2 \right]$, where E_s is the average power of the transmitted symbols.

In the simulations, we compare the proposed MSER-based adaptive DFE with some existing adaptive equalizers with linear and decision feedback structures, which are briefly reviewed as follows. The applied linear equalizers are the normalized LMS (NLMS) equalizer in [25] and [26] and the normalized adaptive minimum bit error rate (NAMBER) equalizer in [19]. By providing the linear adaptive minimum bit error rate (AMBER) equalizer proposed in [17] and [18] with decision feedback structure, the AMBER-DFE is proposed in [22] to achieve better performance. Note the AMBER-DFE in [22] is only developed for BPSK modulation. Its extension to QAM source can be readily written as

$$\mathbf{f}_k = \mathbf{f}_{k-1} + \mu_f \mathcal{I}_k \mathbf{r}_k^* \quad (25)$$

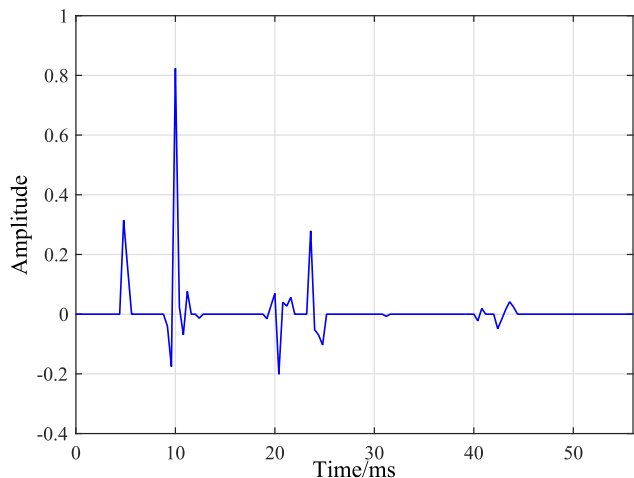


FIGURE 2. The real-value CIR generated from the channel model in [24].

$$\mathbf{b}_k = \mathbf{b}_{k-1} + \mu_b \mathcal{I}_k \hat{\mathbf{s}}_k^* \quad (26)$$

where the indicator function \mathcal{I}_k is given by

$$\mathcal{I}_k = s_{k-D}^R F(s_{k-D}^R y_k^R) + j s_{k-D}^I F(s_{k-D}^I y_k^I) \quad (27)$$

in which $F(t) = (1 - \text{sgn}(t - \tau))/2$ with τ being a predefined threshold. Since the AMBER-DFE has been shown to outperform the MMSE-based DFE, the result of MMSE-based DFE is not presented in the simulations.

To make fair comparison, we set the same total number of taps for all applied equalizers. For the equalizer with decision feedback structure, the numbers of taps for the feedforward and the feedback filters are set to be $N_f = 50$ and $N_b = 100$, respectively. For the equalizer with linear structure, the number of taps is set to be $N = N_f + N_b = 150$. The delay parameter is set to be $D = 30$ for all equalizers.

A. BPSK SOURCE

In this subsection, we consider a time-uncorrelated BPSK input sequence $s_k \in \{\pm 1\}$ for the two underwater acoustic channel models. Fig. 2 shows the applied CIR generated from the channel model in [24], where the sampling interval is $T = 0.4$ ms. After that, we obtain the discrete channel with the maximum delay spread of around 140 symbol periods. Fig. 3 shows the impulse response measured from an underwater acoustic communication experiment, where the receiver is at a distance of 5 km from the transmitter [27]. For the underwater acoustic communication experiment, the sampling rate is 48 kHz, the data transmission rate is 2 kHz, and the maximum delay spread of the channel is about 100 symbol periods. Moreover, we set $w = 0.999$, $\beta = 1$, and $\mathbf{R}_0 = 50\mathbf{I}$ as the initial correlation matrix for the proposed MSER-based adaptive DFE. We set $\mu = \mu_f = \mu_b = 0.8$ for the other equalizers and $\tau = 0.1$ for the AMBER-DFE.

In Figs. 4 and 5, we compare the convergence performance of different equalizers over the channels shown in Figs. 2 and 3, where we show the SER versus the number of symbol iterations under $\text{SNR} = 14$ dB and $\text{SNR} = 12$ dB, respectively. It can be observed from Figs. 4 and 5 that the performance of

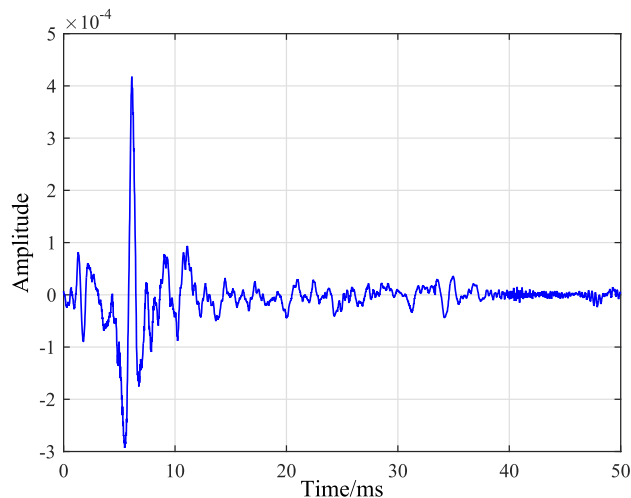


FIGURE 3. The real-value CIR measured from the underwater acoustic communication test [27].

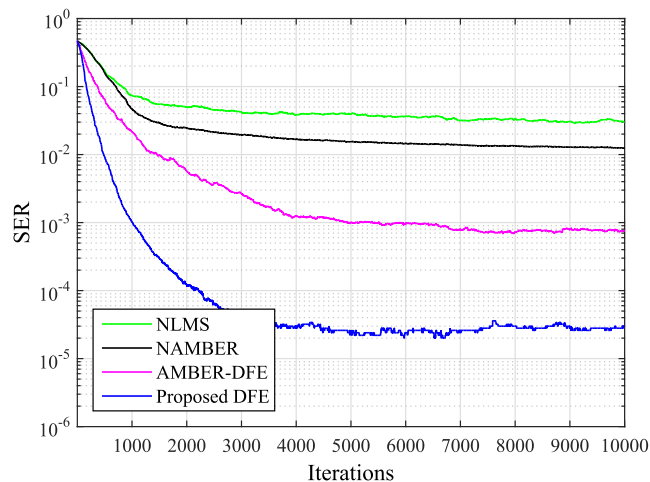


FIGURE 4. Convergence performance comparison of different equalizers with BPSK source under channel of [24], $\text{SNR} = 14$ dB.

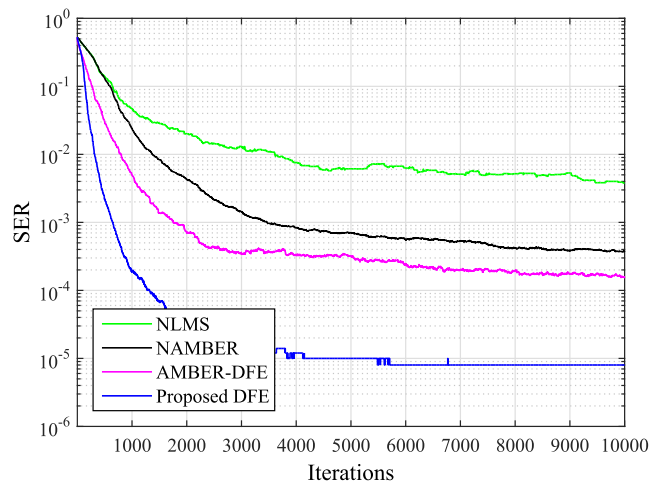


FIGURE 5. Convergence performance comparison of different equalizers with BPSK source under the experimental channel, $\text{SNR} = 12$ dB.

the equalizers with decision feedback structure is much better than that of the equalizers with linear structure. This can be explained by the fact that for the DFEs, the residual ISI at the

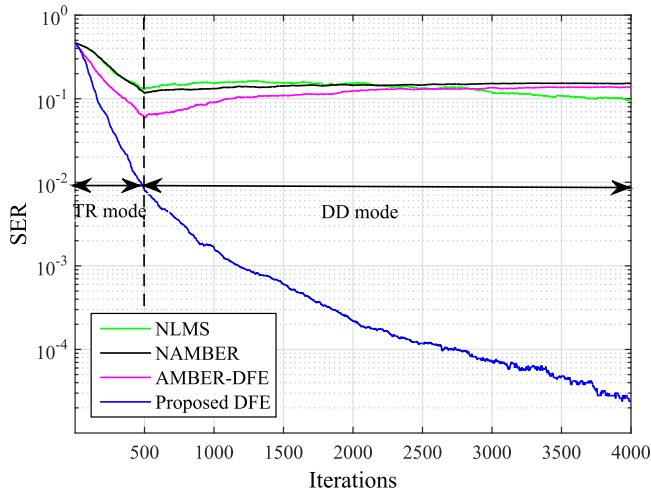


FIGURE 6. Convergence performance comparison of different equalizers with BPSK source under the channel of [24], SNR = 14 dB.

output of the forward equalizer can be effectively mitigated by the feedback filter. Since the feedback filter is applied to remove the part of the ISI from the present estimated symbol, those DFEs can achieve much better SER performance and faster convergence rate over the underwater acoustic channels. Moreover, the proposed MSER-based adaptive DFE outperforms the other equalizers in terms of the steady-state SER performance and the convergence rate, which verifies the effectiveness of the proposed equalizer. Specifically, the proposed MSER-based adaptive DFE converges with only 2000 iterations, which is much faster than the others.

To investigate the ability of equalizers in tracking the CIR, we apply two iteration modes in Fig. 6: the training (TR) mode and the decision-directed (DD) mode. In the TR mode, the transmitted symbols are known to the receiver as training sequence. While in the DD mode, without any priori knowledge of the transmitted symbols at the receiver, those estimated symbols after the equalization are applied as referred signals for coefficient adjustment. Fig. 6 shows the comparison results of the convergence performance over the CIR of Fig. 2 at SNR = 14 dB, where all the equalizers first operate under the TR mode with 500 symbol iterations and then switch to the DD mode. As shown in Fig. 6, the proposed MSER-based adaptive DFE achieves excellent convergence performance in both TR and DD modes. As the outputs of the proposed DFE may be incorrectly estimated as referred signals, the convergence speed in the DD mode is lower than that in the TR mode. However, the convergence performance in the DD mode is satisfactory as the proposed DFE can still converge to a rather low steady-state SER at the order of 10^{-4} after around 2000 iterations in the DD mode. On the other hand, the convergence performance of the other equalizers are less impressive as they converge slowly in the TR mode and thus give rise to the error propagation in the DD mode. Therefore, the proposed MSER-based adaptive DFE is more robust and effective in tracking the CIR, which is more desirable for the underwater acoustic channel.

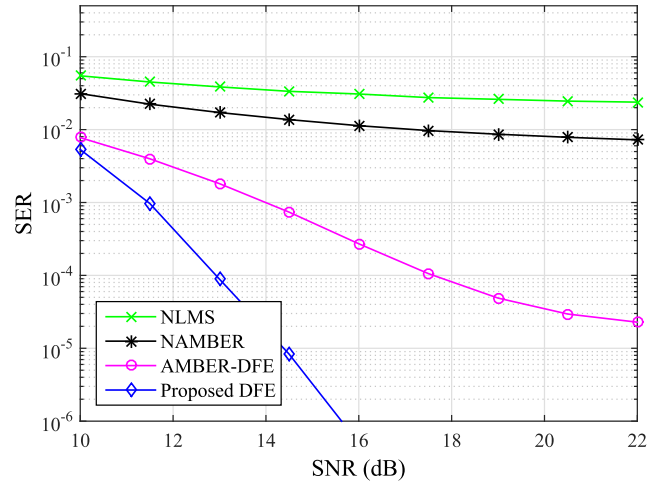


FIGURE 7. BER performance comparison of different equalizers with BPSK source under the channel of [24].

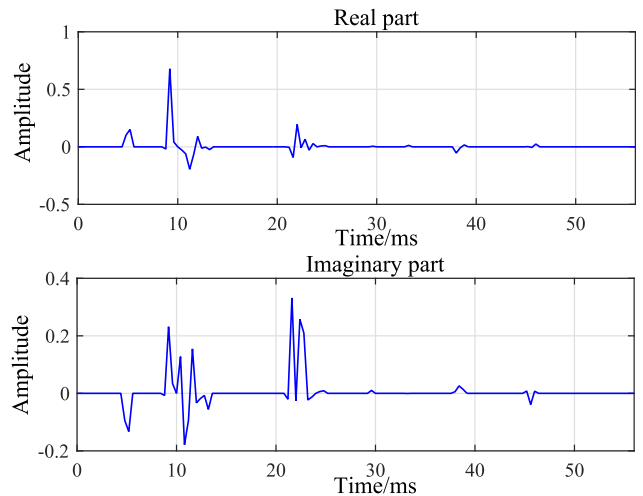


FIGURE 8. The complex CIR from [24].

In Fig. 7, we compare the steady-state SER performance of all the equalizers under different values of SNR. Monte-Carlo simulations are conducted to examine the SER performance of all the equalizers, which are carried out with 10000 iterations to ensure the steady-state SER. Due to low convergence speed shown in the above results, the linear equalizers and the AMBER-DFE can not achieve a desirable steady-state SER performance in the underwater acoustic channel. However, the steady-state SER of the proposed DFE decreases rapidly as the SNR increases, exhibiting outstanding performance in the underwater acoustic channel.

B. 4-QAM SOURCE

Here we consider a time-uncorrelated 4-QAM alphabet under the complex CIR for the simulations. Fig. 8 shows the complex CIR of the underwater acoustic channel with the sampling interval of $T = 0.4$ ms obtained from [24]. Fig. 9 shows the complex CIR of the underwater acoustic channel,

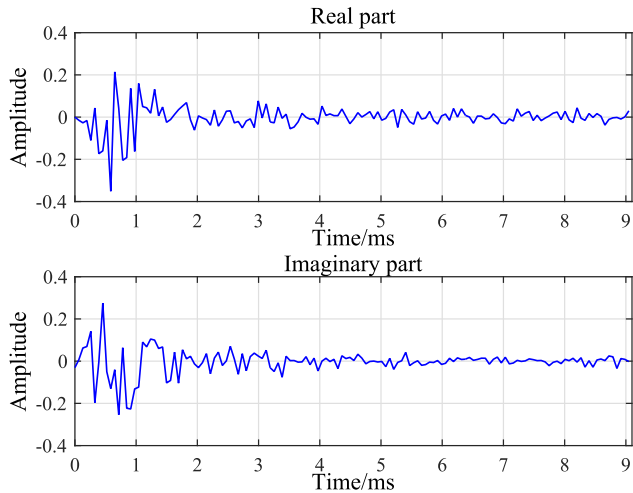


FIGURE 9. The complex CIR measured from the campus lake.

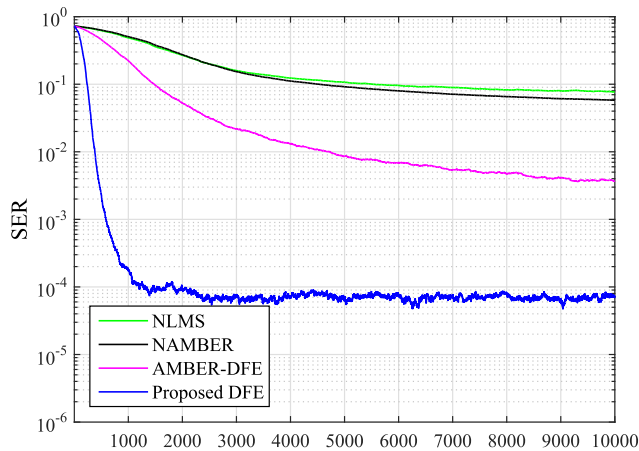


FIGURE 10. Convergence performance of the equalizers with QAM source under the underwater acoustic channel of [24], SNR = 20 dB.

which corresponds to an underwater acoustic link that was measured during the experiment in the campus lake. The data transmission rate is 15 kHz, and the maximum delay spread of the discrete channel is around 140 symbol periods. In the following simulations, we set $w = 0.99$, $\beta = 1$, and $\mathbf{R}_0 = 50\mathbf{I}$ as the initial correlation matrix for the proposed MSER-based adaptive DFE. On the other hand, we set $\mu = \mu_f = \mu_b = 0.2$ for the other equalizers and $\tau = 0.1$ for the AMBER-DFE.

In Figs. 10 and 11, we compare the convergence rates of different equalizers under the complex CIRs shown in Figs. 8 and 9, where we plot SER versus the number of symbol iterations at SNR = 20 dB and SNR = 19 dB, respectively. Similar to the simulation results for the BPSK source, the performance of the equalizers with decision feedback structure is much better than that of the equalizers with linear structure. The equalizers with linear structure suffer from SER performance degradation and slow convergence when the channel encounters a large delay spread. On the other hand, since the DFEs apply the feedback filter to remove part of the ISI from the present estimated symbol, they achieve

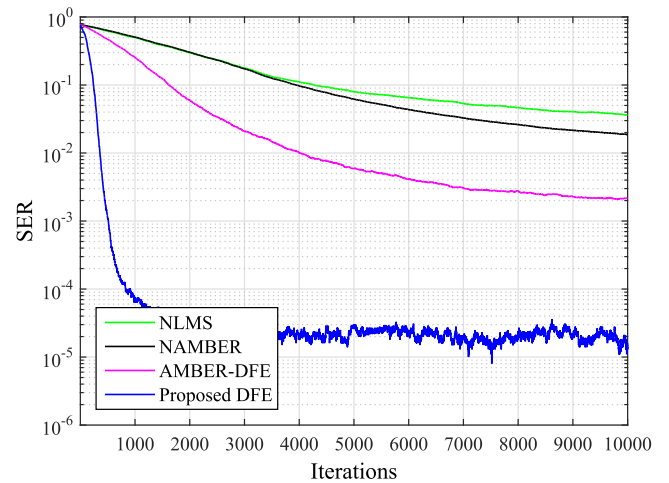


FIGURE 11. Convergence performance of the equalizers with QAM source under the underwater acoustic channel of the campus lake, SNR = 19 dB.

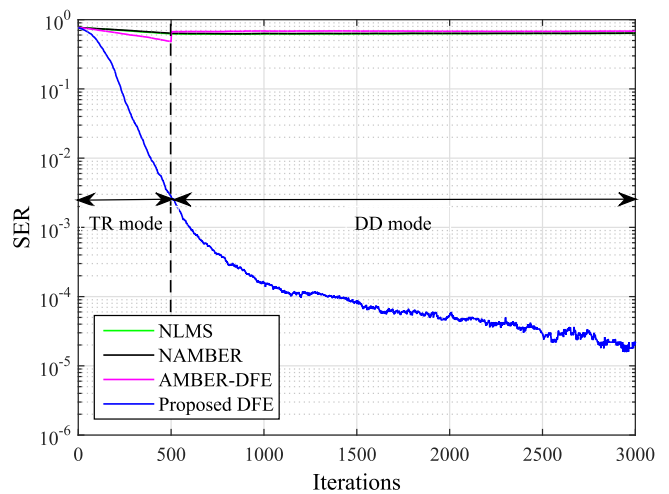


FIGURE 12. Convergence performance of the equalizers with QAM source under the underwater acoustic channel of the campus lake, SNR = 18 dB.

much better SER performance and achieves higher convergence rate in the underwater acoustic channel. Moreover, as shown in Figs. 10 and 11, our proposed MSER-based adaptive DFE not only achieves the best SER performance but also the fastest convergence rate, which is much desirable for the complex underwater acoustic channel.

In Fig. 12, we apply two adaptive modes for each algorithm, namely, the TR mode in which the transmitted symbol s_{k-D} is available at the receiver for the adjustment of the coefficients and the DD mode in which the estimated symbol \hat{s}_{k-D} is used to adjust the coefficients of the equalizers. Fig. 12 shows the learning curves of the four equalizers operating under the two modes, given SNR = 18 dB under the channel of Fig. 9. All the equalizers first operate under the TR mode with 500 symbol iterations and then switch to the DD mode. As shown in Fig. 12, except for the proposed MSER-based adaptive DFE, other equalizers fail to converge due to the error propagation. Specifically, as those equalizers suffer from slow convergence and poor SER performance in the TR mode, they also fail to converge in the DD mode even

with a large number of iterations. However, the proposed DFE achieves excellent convergence performance and SER performance in both TR and DD modes. Although the convergence speed of the proposed DFE in the DD mode is slightly lower than that in the TR mode, the convergence performance in the DD mode is satisfactory as it still can converge quickly to a rather low steady-state SER at the order of 10^{-4} after only 500 iterations in the DD mode. Therefore, the proposed MSER-based adaptive DFE can be regarded as a robust and effective equalization technique for tracking the underwater acoustic channel.

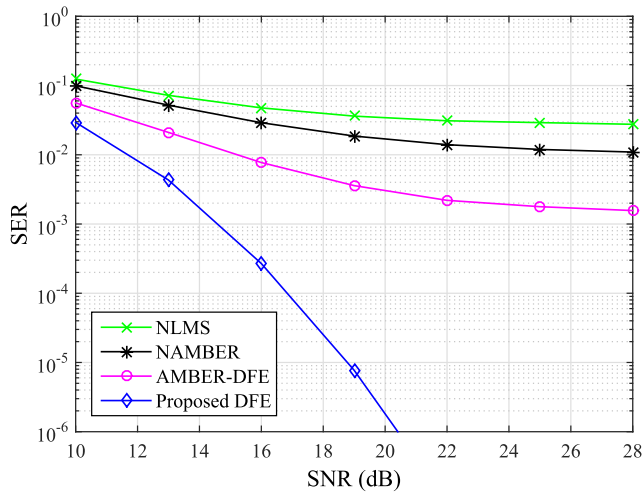


FIGURE 13. SER performance of the equalizers, QAM in the underwater acoustic channel of the campus lake.

The steady-state SER performance with respect to the SNR is depicted in Fig. 13. Monte-Carlo simulations are conducted to examine the SER performance of all the equalizers, where each equalizer is carried out 10 000 iterations to achieve its steady-state SER. As seen from the figure, the steady-state SERs of the linear equalizers and the AMBER-DFE decrease slowly as the SNR increases, nearly creating an error floor. This can be explained by the fact that as the underwater acoustic channel has a large delay spread, the linear equalizers and the AMBER-DFE suffer from the slow convergence performance while the convergence rate of these equalizers do not improve much as the SNR increases. Therefore, limited by the low convergence rate in the underwater acoustic channel with large delay spread, these equalizers cannot converge to the desirable steady-state SER performance. In contrast, the steady-state SER and convergence performance of the proposed MSER-based adaptive DFE is much more desirable. As shown in Fig. 13, the steady-state SER of the proposed DFE decreases rapidly as the SNR increases, verifying the superiority of this equalization algorithm in compensating for the underwater acoustic channel with large delay spread.

V. CONCLUSION

In this paper, we have developed a novel equalization algorithms based on MSER criterion with decision feedback

structure to accelerate the convergence speed and achieve rather low steady-state SER. In particular, the superior performance of the proposed MSER-based adaptive DFE comes at the expense of higher computational complexity. However, in many communication systems with large delay spread and fast fading, such as underwater acoustic communications, the transmission rate of signals is much slower than that in terrestrial communications and thus is tolerant to higher computational complexity. Therefore, it can be a smart choice for this type of communication systems to enhance the convergence rate of equalizer at the cost of higher computational complexity.

APPENDIX A DERIVATION OF (9)

The derivative of $J(\mathbf{c}_k)$ in (8) with respect to \mathbf{c}_k is given by

$$\frac{\partial J(\mathbf{c}_k)}{\partial \mathbf{c}_k} = 2(\mathbf{c}_k - \mathbf{c}_{k-1}) + \beta \sum_{i=D}^k \lambda_i \tanh'(\beta \mathbf{c}_k^T \mathbf{v}_i) \mathbf{v}_i. \quad (28)$$

Setting the derivative in (28) to zero yields

$$\mathbf{c}_k = \mathbf{c}_{k-1} - \frac{1}{2} \beta \sum_{i=D}^k \lambda_i \tanh'(\beta \mathbf{c}_k^T \mathbf{v}_i) \mathbf{v}_i. \quad (29)$$

By multiplying vector \mathbf{v}_j^T to both sides of (7), we have

$$\left(\text{sgn}(\beta \mathbf{c}_k^T \mathbf{v}_j) - s_{j-D} \right) \mathbf{v}_j^T = \mathbf{0}, \quad j = k, k-1, \dots, D. \quad (30)$$

Substituting (29) into the constraint of (30) with $\text{sgn}(x)$ replaced by $\tanh(\beta x)$ yields

$$\begin{aligned} \tanh \left(\beta \mathbf{c}_{k-1}^T \mathbf{v}_j - \frac{1}{2} \beta^2 \sum_{i=D}^k \lambda_i \tanh'(\beta \mathbf{c}_k^T \mathbf{v}_i) \mathbf{v}_i^T \mathbf{v}_j \right) \mathbf{v}_j^T \\ = s_{j-D} \mathbf{v}_j^T \end{aligned} \quad (31)$$

where $j = k, k-1, \dots, D$. The second item inside of $\tanh(\cdot)$ would take a small value when the channel distortion can be well compensated for by the equalizer. By resorting to the first-order Taylor series, we make an approximation of $\tanh(x + \Delta)$ with Δ being a tiny value, i.e., $\tanh(x + \Delta) \approx \tanh(x) + \tanh'(x)\Delta$. Therefore, (31) can be well approximated by

$$\begin{aligned} s_{j-D} \mathbf{v}_j^T &= \tanh(\beta \mathbf{c}_{k-1}^T \mathbf{v}_j) \mathbf{v}_j^T - \frac{1}{2} \beta^2 \tanh'(\beta \mathbf{c}_{k-1}^T \mathbf{v}_j) \\ &\quad \times \sum_{i=D}^k \lambda_i \tanh'(\beta \mathbf{c}_k^T \mathbf{v}_i) \mathbf{v}_i^T \mathbf{v}_j \mathbf{v}_j^T \end{aligned} \quad (32)$$

where $j = k, k-1, \dots, D$. Note that when the channel is well compensated for, we have $\beta \tanh'(\beta \mathbf{c}_{k-1}^T \mathbf{v}_j) \approx \beta \tanh'(\beta)$. Then we obtain

$$\begin{aligned} \frac{1}{2} \beta \sum_{i=D}^k \lambda_i \tanh'(\beta \mathbf{c}_k^T \mathbf{v}_i) \mathbf{v}_i^T \left(\mathbf{v}_j \mathbf{v}_j^T \right) \\ = \frac{(\tanh(\beta \mathbf{c}_{k-1}^T \mathbf{v}_j) - s_{j-D}) \mathbf{v}_j^T}{\beta \tanh'(\beta)} \end{aligned} \quad (33)$$

where $j = k, k - 1, \dots, D$. Here we introduce a forgetting factor w to combine multiple equations of (33)

$$-\frac{1}{2}\beta \sum_{i=D}^k \lambda_i \tan h'(\beta \mathbf{c}_k^T \mathbf{v}_i) \mathbf{v}_i^T \sum_{j=D}^k w^{k-j} (\mathbf{v}_j \mathbf{v}_j^T) = -\sum_{j=D}^k w^{k-j} \frac{(\tanh(\beta \mathbf{c}_{k-1}^T \mathbf{v}_j) - s_{j-D}) \mathbf{v}_j^T}{\beta \tan h'(\beta)}. \quad (34)$$

Note that (34) can be regarded as the polynomial of w , which is equivalent to equations of (33) [28, Ch. 15.1]. Then, we add $\mathbf{c}_{k-1}^T \sum_{j=D}^k w^{k-j} (\mathbf{v}_j \mathbf{v}_j^T)$ to both sides of (34) and obtain

$$\left(\mathbf{c}_{k-1}^T - \frac{1}{2}\beta \sum_{i=D}^k \lambda_i \tan h'(\beta \mathbf{c}_k^T \mathbf{v}_i) \mathbf{v}_i^T \right) \sum_{j=D}^k w^{k-j} (\mathbf{v}_j \mathbf{v}_j^T) = \sum_{j=D}^k w^{k-j} \left(-\frac{(\tanh(\beta \mathbf{c}_{k-1}^T \mathbf{v}_j) - s_{j-D}) \mathbf{v}_j^T}{\beta \tan h'(\beta)} + \mathbf{c}_{k-1}^T (\mathbf{v}_j \mathbf{v}_j^T) \right). \quad (35)$$

After substituting \mathbf{c}_k^T of (29) into the left side of (35), we can simplify (35) as follows:

$$\begin{aligned} & \mathbf{c}_k^T \sum_{j=D}^k w^{k-j} (\mathbf{v}_j \mathbf{v}_j^T) \\ &= \sum_{j=D}^k w^{k-j} \left(-\frac{(\tanh(\beta \mathbf{c}_{k-1}^T \mathbf{v}_j) - s_{j-D}) \mathbf{v}_j^T}{\beta \tan h'(\beta)} + \mathbf{c}_{k-1}^T (\mathbf{v}_j \mathbf{v}_j^T) \right) \\ &= w \sum_{j=D}^{k-1} w^{k-1-j} \left(-\frac{(\tanh(\beta \mathbf{c}_{k-2}^T \mathbf{v}_j) - s_{j-D}) \mathbf{v}_j^T}{\beta \tan h'(\beta)} + \mathbf{c}_{k-2}^T (\mathbf{v}_j \mathbf{v}_j^T) \right) \\ &\quad - \frac{(\tanh(\beta \mathbf{c}_{k-1}^T \mathbf{v}_k) - s_{k-D}) \mathbf{v}_k^T}{\beta \tan h'(\beta)} + \mathbf{c}_{k-1}^T (\mathbf{v}_k \mathbf{v}_k^T) \\ &= w \mathbf{c}_{k-1}^T \sum_{j=D}^{k-1} w^{k-1-j} (\mathbf{v}_j \mathbf{v}_j^T) \\ &\quad - \frac{(\tanh(\beta \mathbf{c}_{k-1}^T \mathbf{v}_k) - s_{k-D}) \mathbf{v}_k^T}{\beta \tan h'(\beta)} + \mathbf{c}_{k-1}^T (\mathbf{v}_k \mathbf{v}_k^T) \\ &= \mathbf{c}_{k-1}^T \left(\sum_{j=D}^k w^{k-j} (\mathbf{v}_j \mathbf{v}_j^T) - \mathbf{v}_k \mathbf{v}_k^T \right) \\ &\quad - \frac{(\tanh(\beta \mathbf{c}_{k-1}^T \mathbf{v}_k) - s_{k-D}) \mathbf{v}_k^T}{\beta \tan h'(\beta)} + \mathbf{c}_{k-1}^T (\mathbf{v}_k \mathbf{v}_k^T) \\ &= \mathbf{c}_{k-1}^T \sum_{j=D}^k w^{k-j} (\mathbf{v}_j \mathbf{v}_j^T) - \frac{(\tanh(\beta \mathbf{c}_{k-1}^T \mathbf{v}_k) - s_{k-D}) \mathbf{v}_k^T}{\beta \tan h'(\beta)}. \end{aligned} \quad (36)$$

Define

$$\mathbf{R}_k = \sum_{j=D}^k w^{k-j} (\mathbf{v}_j \mathbf{v}_j^T), \quad (37)$$

as the signal correlation matrix and

$$\zeta_k = \frac{(\tanh(\beta \mathbf{c}_{k-1}^T \mathbf{v}_k) - s_{k-D})}{\beta \tan h'(\beta)} \quad (38)$$

as the error indicator of symbol detection. By right multiplying the inverse of matrix \mathbf{R}_k , i.e., \mathbf{R}_k^{-1} and taking the transpose operation of (36), we can obtain the following adaptive algorithm:

$$\mathbf{c}_k = \mathbf{c}_{k-1} - \zeta_k \mathbf{R}_k^{-1} \mathbf{v}_k \quad (39)$$

completing the derivation.

APPENDIX B DERIVATION OF (19)

The derivative of $J(\bar{\mathbf{c}}_k)$ in (18) with respect to $\bar{\mathbf{c}}_k$ is given by

$$\begin{aligned} \frac{\partial J(\bar{\mathbf{c}}_k)}{\partial \bar{\mathbf{c}}_k} &= 2(\bar{\mathbf{c}}_k - \bar{\mathbf{c}}_{k-1}) \\ &+ \beta \sum_{i=D}^k \lambda_i \left(\tanh(\beta (\bar{\mathbf{c}}_k^T \bar{\mathbf{v}}_i - \Re\{s_{i-D}\} + d)) \right. \\ &\quad \left. + \tanh(\beta (\bar{\mathbf{c}}_k^T \bar{\mathbf{v}}_i - \Re\{s_{i-D}\} - d)) \right) \bar{\mathbf{v}}_i. \end{aligned} \quad (40)$$

Set the derivative in (40) to zero and we obtain

$$\begin{aligned} \bar{\mathbf{c}}_k &= \bar{\mathbf{c}}_{k-1} - \frac{1}{2}\beta \sum_{i=D}^k \lambda_i \left(\tanh(\beta (\bar{\mathbf{c}}_k^T \bar{\mathbf{v}}_i - \Re\{s_{i-D}\} + d)) \right. \\ &\quad \left. + \tanh(\beta (\bar{\mathbf{c}}_k^T \bar{\mathbf{v}}_i - \Re\{s_{i-D}\} - d)) \right) \bar{\mathbf{v}}_i. \end{aligned} \quad (41)$$

Left multiplying $\bar{\mathbf{v}}_j^T$ to both sides of the equation (41) yields

$$\begin{aligned} & \text{sgn}(\bar{\mathbf{c}}_k^T \bar{\mathbf{v}}_j - \Re\{s_{j-D}\} + d) \bar{\mathbf{v}}_j^T \\ &+ \text{sgn}(\bar{\mathbf{c}}_k^T \bar{\mathbf{v}}_j - \Re\{s_{j-D}\} - d) \bar{\mathbf{v}}_j^T = 0 \end{aligned} \quad (42)$$

where $j = k, k - 1, \dots, D$. Substituting (41) into the constraint of (42) with $\text{sgn}(x)$ replaced by $\tanh(\beta x)$, and similarly approximating $\tanh(x + \Delta)$ with the first-order Taylor series yields

$$\begin{aligned} & \frac{1}{2}\beta \sum_{i=D}^k \lambda_i \left(\tanh(\beta (\bar{\mathbf{c}}_k^T \bar{\mathbf{v}}_j - \Re\{s_{j-D}\} + d)) \right. \\ & \quad \left. + \tanh(\beta (\bar{\mathbf{c}}_k^T \bar{\mathbf{v}}_j - \Re\{s_{j-D}\} - d)) \right) \bar{\mathbf{v}}_i^T \bar{\mathbf{v}}_j \bar{\mathbf{v}}_j^T \\ &= \frac{\tanh(\beta (\Omega_R + 1)) \bar{\mathbf{v}}_j^T + \tanh(\beta (\Omega_R - 1)) \bar{\mathbf{v}}_j^T}{\beta (\tan h'(\beta (\Omega_R + 1)) + \tan h'(\beta (\Omega_R - 1)))} \end{aligned} \quad (43)$$

where $j = k, k - 1, \dots, D$, and $\Omega_R = \bar{\mathbf{c}}_{k-1}^T \bar{\mathbf{r}}_k - \Re\{s_{k-D}\}$. If the channel distortion can be well compensated for by the equalizer, we have $\Omega_R \approx 0$ and consequently $\beta \tan h'(\beta (\Omega_R \pm 1)) \approx \beta \tan h'(\beta)$ can be considered as a constant in (43).

We also introduce a forgetting factor w to combine multiple equations of (43), yielding

$$\begin{aligned}
 & -\frac{1}{2}\beta \sum_{i=D}^k \lambda_i \left(\tanh \left(\beta (\bar{\mathbf{c}}_k^T \bar{\mathbf{v}}_i - \Re\{s_{j-D}\} + d) \right) \right. \\
 & \quad \left. + \tanh \left(\beta (\bar{\mathbf{c}}_k^T \bar{\mathbf{v}}_i - \Re\{s_{i-D}\} - d) \right) \right) \bar{\mathbf{v}}_i^T \sum_{j=D}^k w^{k-j} \left(\bar{\mathbf{v}}_j \bar{\mathbf{v}}_j^T \right) \\
 & = -\sum_{j=D}^k w^{k-j} \frac{\tanh(\beta(\Omega_R + 1)) + \tanh(\beta(\Omega_R - 1))}{2\beta \tanh'(\beta)} \bar{\mathbf{v}}_j^T.
 \end{aligned} \tag{44}$$

Then we add $\bar{\mathbf{c}}_{k-1}^T \sum_{j=D}^k w^{k-j} (\bar{\mathbf{v}}_j \bar{\mathbf{v}}_j^T)$ to both sides of (44), and substitute

$$\begin{aligned}
 \bar{\mathbf{c}}_k^T & = \bar{\mathbf{c}}_{k-1}^T - \frac{1}{2}\beta \sum_{i=D}^k \lambda_i \left(\tanh(\beta(\bar{\mathbf{c}}_k^T \bar{\mathbf{v}}_i - \Re\{s_{i-D}\} + d) \right. \\
 & \quad \left. + \tanh(\beta(\bar{\mathbf{c}}_k^T \bar{\mathbf{v}}_i - \Re\{s_{i-D}\} - d)) \right) \bar{\mathbf{v}}_i^T
 \end{aligned}$$

into the left side of (44), yielding

$$\begin{aligned}
 & \bar{\mathbf{c}}_k^T \sum_{j=D}^k w^{k-j} (\bar{\mathbf{v}}_j \bar{\mathbf{v}}_j^T) \\
 & = \sum_{j=D}^k w^{k-j} \left(-\frac{\tanh(\beta(\Omega_R + d)) + \tanh(\beta(\Omega_R - d))}{2\beta \tanh'(\beta)} \bar{\mathbf{v}}_j^T \right. \\
 & \quad \left. + \bar{\mathbf{c}}_{k-1}^T (\bar{\mathbf{v}}_j \bar{\mathbf{v}}_j^T) \right) \\
 & = w \sum_{j=D}^{k-1} w^{k-1-j} \left(-\frac{\tanh(\beta(\Omega_R + d)) + \tanh(\beta(\Omega_R - d))}{2\beta \tanh'(\beta)} \bar{\mathbf{v}}_j^T \right. \\
 & \quad \left. + \bar{\mathbf{c}}_{k-2}^T (\bar{\mathbf{v}}_j \bar{\mathbf{v}}_j^T) \right) \\
 & \quad - \frac{\tanh(\beta(\Omega_R + d)) + \tanh(\beta(\Omega_R - d))}{2\beta \tanh'(\beta)} \bar{\mathbf{v}}_k^T + \bar{\mathbf{c}}_{k-1}^T (\bar{\mathbf{v}}_k \bar{\mathbf{v}}_k^T) \\
 & = w \bar{\mathbf{c}}_{k-1}^T \sum_{j=D}^{k-1} w^{k-1-j} (\bar{\mathbf{v}}_j \bar{\mathbf{v}}_j^T) + \bar{\mathbf{c}}_{k-1}^T (\bar{\mathbf{v}}_k \bar{\mathbf{v}}_k^T) \\
 & \quad - \frac{\tanh(\beta(\Omega_R + d)) + \tanh(\beta(\Omega_R - d))}{2\beta \tanh'(\beta)} \bar{\mathbf{v}}_k^T \\
 & = \bar{\mathbf{c}}_{k-1}^T \left(\sum_{j=D}^k w^{k-j} (\bar{\mathbf{v}}_j \bar{\mathbf{v}}_j^T) - \bar{\mathbf{v}}_k \bar{\mathbf{v}}_k^T \right) + \bar{\mathbf{c}}_{k-1}^T (\bar{\mathbf{v}}_k \bar{\mathbf{v}}_k^T) \\
 & \quad - \frac{\tanh(\beta(\Omega_R + d)) + \tanh(\beta(\Omega_R - d))}{2\beta \tanh'(\beta)} \bar{\mathbf{v}}_k^T \\
 & = \bar{\mathbf{c}}_{k-1}^T \sum_{j=D}^k w^{k-j} (\bar{\mathbf{v}}_j \bar{\mathbf{v}}_j^T) \\
 & \quad - \frac{\tanh(\beta(\Omega_R + d)) + \tanh(\beta(\Omega_R - d))}{2\beta \tanh'(\beta)} \bar{\mathbf{v}}_k^T.
 \end{aligned} \tag{45}$$

Here the signal correlation matrix is defined by

$$\bar{\mathbf{R}}_k = \sum_{j=D}^k w^{k-j} (\bar{\mathbf{v}}_j \bar{\mathbf{v}}_j^T) \tag{46}$$

and the real part of ζ_k denotes the real part of the error indicator of symbol detection, which is given by

$$\Re\{\zeta_k\} = \frac{\tanh(\beta(\Omega_R + d)) + \tanh(\beta(\Omega_R - d))}{2\beta \tanh'(\beta)}. \tag{47}$$

After right multiplying the inverse of matrix $\bar{\mathbf{R}}_k$, i.e., $\bar{\mathbf{R}}_k^{-1}$, and taking the transpose operation of (45), we obtain the following adaptive algorithm for the real part:

$$\bar{\mathbf{c}}_k = \bar{\mathbf{c}}_{k-1} - \Re\{\zeta_k\} \bar{\mathbf{R}}_k^{-1} \bar{\mathbf{v}}_k \tag{48}$$

completing the derivation.

REFERENCES

- [1] J. Heidemann, M. Stojanovic, and M. Zorzi, "Underwater sensor networks: Applications, advances and challenges," *Philos. Trans. Roy. Soc. London A, Math. Phys. Sci.*, vol. 370, no. 1958, pp. 158–175, Jan. 2012.
- [2] Y. R. Zheng, J. Wu, and C. Xiao, "Turbo equalization for single-carrier underwater acoustic communications," *IEEE Commun. Mag.*, vol. 53, no. 11, pp. 79–87, Nov. 2015.
- [3] A. C. Singer, J. K. Nelson, and S. S. Kozat, "Signal processing for underwater acoustic communications," *IEEE Commun. Mag.*, vol. 47, no. 1, pp. 90–96, Jan. 2009.
- [4] D. B. Kilfoyle and A. B. Baggeroer, "The state of the art in underwater acoustic telemetry," *IEEE J. Ocean. Eng.*, vol. 25, no. 1, pp. 4–27, Jan. 2000.
- [5] N. Iruthayanathan, K. S. Vishvakshenan, and V. Rajendran, "Performance of spread spectrum based multi-carrier system in underwater communication using transmitter pre-processing," *IEEE Access*, vol. 4, pp. 5128–5134, Jul. 2016.
- [6] X. Zhang, K. Song, C. Li, and L. Yang, "Parameter estimation for multi-scale multi-lag underwater acoustic channels based on modified particle swarm optimization algorithm," *IEEE Access*, vol. 5, pp. 4808–4820, Mar. 2017.
- [7] M. Stojanovic, J. Catipovic, and J. G. Proakis, "Adaptive multichannel combining and equalization for underwater acoustic communications," *J. Acoust. Soc. Amer.*, vol. 94, no. 3, pp. 1621–1631, Sep. 1993.
- [8] J. G. Proakis, "Adaptive equalization techniques for acoustic telemetry channels," *IEEE J. Ocean. Eng.*, vol. 16, no. 1, pp. 21–31, Jan. 1991.
- [9] S. Weib, S. R. Dooley, R. W. Stewart, and A. K. Nandi, "Adaptive equalisation in oversampled subbands," *Electron. Lett.*, vol. 34, no. 15, pp. 1452–1453, Jul. 1998.
- [10] K. Vanbleu, M. Moonen, and G. Leus, "Linear and decision-feedback per tone equalization for DMT-based transmission over IIR channels," *IEEE Trans. Signal Process.*, vol. 54, no. 1, pp. 258–273, Jan. 2006.
- [11] J. Taot, Y. R. Zheng, C. Xiao, and T. C. Yang, "Iterative block decision feedback equalization for MIMO underwater acoustic communications," in *Proc. MTS/IEEE Int. Oceans Conf.*, Biloxi, MS, USA, Oct. 2009, pp. 1–6.
- [12] T. C. Yang, "Correlation-based decision-feedback equalizer for underwater acoustic communications," *IEEE J. Ocean. Eng.*, vol. 30, no. 4, pp. 865–880, Oct. 2005.
- [13] H. Yu, M.-S. Kim, T. Jeori, and S.-K. Lee, "Equalization scheme for OFDM systems in long delay spread channels," in *Proc. 15th IEEE PIMRC*, vol. 2. Barcelona, Spain, Sep. 2004, pp. 1297–1301.
- [14] J. W. Choi, T. J. Riedl, K. Kim, A. C. Singer, and J. C. Preisig, "Adaptive linear turbo equalization over doubly selective channels," *IEEE J. Ocean. Eng.*, vol. 36, no. 4, pp. 473–489, Oct. 2011.
- [15] J. Tao, Y. R. Zheng, C. Xiao, and T. C. Yang, "Robust MIMO underwater acoustic communications using turbo block decision-feedback equalization," *IEEE J. Ocean. Eng.*, vol. 35, no. 4, pp. 948–960, Oct. 2010.
- [16] S. Chen, S. Tan, L. Xu, and L. Hanzo, "Adaptive minimum error-rate filtering design: A review," *Signal Process.*, vol. 88, no. 7, pp. 1671–1697, Jul. 2008.

[17] C.-C. Yeh and J. R. Barry, "Adaptive minimum bit-error rate equalization for binary signaling," *IEEE Trans. Commun.*, vol. 48, no. 7, pp. 1226–1235, Jul. 2000.

[18] C.-C. Yeh and J. R. Barry, "Adaptive minimum symbol-error rate equalization for quadrature-amplitude modulation," *IEEE Trans. Signal Process.*, vol. 51, no. 12, pp. 3263–3269, Dec. 2003.

[19] M. Gong, F. Chen, H. Yu, Z. Lu, and L. Hu, "Normalized adaptive channel equalizer based on minimal symbol-error-rate," *IEEE Trans. Commun.*, vol. 61, no. 4, pp. 1374–1383, Apr. 2013.

[20] S. Chen, L. Hanzo, and B. Mulgrew, "Adaptive minimum symbol-error-rate decision feedback equalization for multilevel pulse-amplitude modulation," *IEEE Trans. Signal Process.*, vol. 52, no. 7, pp. 2092–2101, Jul. 2004.

[21] B. Mulgrew and S. Chen, "Adaptive minimum-BER decision feedback equalisers for binary signalling," *Signal Process.*, vol. 81, no. 7, pp. 1479–1489, Jul. 2001.

[22] R. C. D. Lamare and R. Sampaio-Neto, "Adaptive MBER decision feedback multiuser receivers in frequency selective fading channels," *IEEE Commun. Lett.*, vol. 7, no. 2, pp. 73–75, Feb. 2003.

[23] W. W. Hager, "Updating the inverse of a matrix," *SIAM Rev.*, vol. 31, no. 2, pp. 221–239, Jun. 1989.

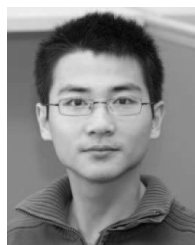
[24] A. Song, J. Senne, M. Badiy, and K. B. Smith, "Underwater acoustic communication channel simulation using parabolic equation," in *Proc. 8th ACM Int. Conf. Underwater Netw. Syst.*, Seattle, WA, USA, Dec. 2011, Art. no. 2.

[25] D. T. M. Slock, "On the convergence behavior of the LMS and the normalized LMS algorithms," *IEEE Trans. Signal Process.*, vol. 41, no. 9, pp. 2811–2825, Sep. 1993.

[26] M. Tarrab and A. Feuer, "Convergence and performance analysis of the normalized LMS algorithm with uncorrelated Gaussian data," *IEEE Trans. Inf. Theory*, vol. IT-34, no. 4, pp. 680–691, Jul. 1988.

[27] F. Qu, X. Nie, and W. Xu, "A two-stage approach for the estimation of doubly spread acoustic channels," *IEEE J. Ocean. Eng.*, vol. 40, no. 1, pp. 131–143, Jan. 2015.

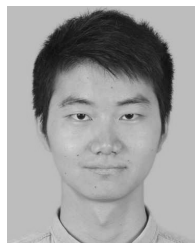
[28] M. Eie and S.-T. Chang, *A Course on Abstract Algebra*. Singapore: World Scientific, 2010.



BEIXIONG ZHENG received the B.S. degree from the South China University of Technology, Guangzhou, China, in 2013, where he is currently pursuing the Ph.D. degree.

From 2015 to 2016, he was a Visiting Student Research Collaborator with Columbia University, New York, NY, USA. His recent research interests include spatial modulation, non-orthogonal multiple access, and pilot multiplexing techniques. He received the Best Paper Award from the IEEE

International Conference on Computing, Networking and Communications 2016.



QIANG LI received the B.S. degree from the Inner Mongolia University of Science and Technology, Baotou, China, in 2013, and the M.S. degree from the Nanjing University of Aeronautics and Astronautics, Nanjing, China, in 2016. He is currently pursuing the Ph.D. degree with the South China University of Technology, Guangzhou, China. His recent research interests include multi-in multi-out systems, index modulation, and OFDM.



MIAOWEN WEN (M'14) received the B.S. degree from Beijing Jiaotong University, Beijing, China, in 2009, and the Ph.D. degree from Peking University, Beijing, in 2014. From 2012 to 2013, he was a Visiting Student Research Collaborator with Princeton University, Princeton, NJ, USA. He is currently an Associate Professor with the South China University of Technology, Guangzhou, China. He has authored a book and over 70 papers in refereed journals and conference proceedings.

His research interests include index modulation and non-orthogonal multiple access techniques.

Dr. Wen received the Best Paper Award from the IEEE International Conference on Intelligent Transportation Systems Telecommunications in 2012, the IEEE International Conference on Intelligent Transportation Systems in 2014, and the IEEE International Conference on Computing, Networking and Communications in 2016. He received the Excellent Doctoral Dissertation Award from Peking University. He currently serves as an Associate Editor for the IEEE Access and on the Editorial Board of *EURASIP Journal on Wireless Communications and Networking* and *ETRI Journal*.



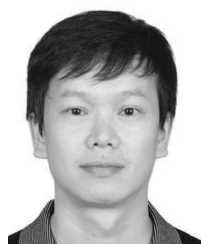
YUN LIU received the B.S. degree in electronic and information engineering from Nanchang University, Nanchang, China, in 2004, and the M.S. degree in radio physics from Sun Yat-sen University, Guangzhou, China, in 2006. He is currently pursuing the Ph.D. degree with the South China University of Technology, Guangzhou.

He is currently a Lecturer with the School of Information Science and Technology, Zhongkai University of Agriculture and Engineering, Guangzhou. His recent research interests include underwater acoustic communications and index modulation.



FEI JI (M'06) received the Ph.D. degree from the South China University of Technology in 1998. She was a Lecturer with the South China University of Technology. From 2003 to 2008, she was an Associate Professor. From 2001 to 2002, she was a Research Assistant with the City University of Hong Kong. She was a Senior Research Associate in 2005. From 2009 to 2010, she was a Visiting Scholar with the University of Waterloo. She is currently a Full-Time Professor with the

South China University of Technology. Her research focuses on wireless communication system and networking.



FANGJIONG CHEN (M'06) received the B.S. degree in electronics and information technology from Zhejiang University, Hangzhou, China, in 1997, and the Ph.D. degree in communication and information engineering from the South China University of Technology, Guangzhou, China, in 2002. He was with the School of Electronics and Information Engineering, South China University of Technology. From 2002 to 2005, he was a Lecturer, and from 2005 to 2011, he was an Associate Professor with the South China University of Technology.

He is currently a Full-Time Professor with the School of Electronics and Information Engineering, South China University of Technology. He is the Director with the Department of Underwater Detection and Imaging, Mobile Ultrasonic Detection National Research Center of Engineering Technology. His research focuses on signal detection and estimation, array signal processing, and wireless communication.

Prof. Chen received the National Science Fund for Outstanding Young Scientists in 2013. He was elected in the New Century Excellent Talent Program of MOE, China, in 2012.



SHAO LIN received the B.S. and M.S. degrees from the South China University of Technology, Guangzhou, China, in 2013 and 2016, respectively, where she is currently pursuing the Ph.D. degree. Her recent research interests include multi-in multi-out systems, OFDM, and non-orthogonal multiple access.